

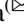





Improvement of the Information Technology Basis for Aerospace Monitoring of the Sea Shelf for the Search for Hydrocarbon Deposits in the Optical Spectral Range

Oleksandr Fedorovskyi , Olga Sedlerova  , and Anna Khyzhniak 

Scientific Center for Aerospace Research of the Earth of the Institute of Geological Sciences of the National Academy of Sciences of Ukraine, Olesia Honchara Street, Kyiv 01054, Ukraine
sedlerova@casre.kiev.ua

Abstract. The paper presents an analysis of satellite images of temperature anomalies over the Schmidt and Golitsyn fields. An analysis of the state of the aquatic environment under various hydrological and hydrophysical conditions has been carried out. Firstly, with hydrology close to isotherm and intense fluid flow, this can be an airlift process, i.e., the removal of cold deep waters by a fluid flow to the sea surface. Second, if there are density gradients in the stratified water column, migrating fluids also cause the formation of internal waves propagating towards the water surface and interacting with it. Thirdly, in hydrology with a pronounced thermocline, the flow of fluids, reaching it, causes fluctuations in density and temperature in it, propagating from the area of disturbance to the free water surface in the form of internal waves (IW). The frequency of these waves is known as the Brent-Waisell frequency. For further detailed study of the process of formation of temperature anomalies on the free water surface over hydrocarbon deposits, the result of modeling this process obtained earlier at different times from the board of ships and offshore platforms in the Black, Japanese and Barents Seas was used. After processing and analyzing the results of marine physical modeling of the formation of temperature anomalies on the sea surface, a unique statistical material was obtained in different marine areas, hydrology and seasons. Among other things, several dozens of different Haralik parameters were tested and the five most informative of them were selected for further use: Contrast, Sum Variance, Sum Entropy, Entropy and Difference Entropy. As a result of the research, new technological methods for searching and predicting explosive deposits were proposed.

Keywords: aerospace monitoring · multispectral satellite imagery data · structural and textural parameters · hydrocarbon deposits

1 Introduction

Interest in the study of hydrophysics and hydrodynamics of sea surface temperature and its distribution in the surface layer of water are due to two main factors. First, it is energy-mass exchange between the atmosphere and the ocean. The spatial distribution of temperature is important in the simulation of large-scale processes in climate models, which is essential for weather forecasting and assessments of long-term climate changes. The second factor is interest in the hydrodynamics of the near-surface layer of water, which can be used as one of the informative features when searching for hydrocarbon deposits in the shelf zone. The water surface for aerospace monitoring is the natural integrator of information, which allows you to detect processes occurring not only on the sea surface, but also in the water column and bottom space. Information about the temperature of the surface layer of the sea is carried by its infrared thermal radiation, the intensity of which is related to the usual thermodynamic temperature by the well-known Stefan-Boltzmann law [1].

The purpose of the research is to reveal the hydrophysical and geological features of the sea surface in the optical spectral range, which form informative features for aerospace geomonitoring of the search for hydrocarbon deposits and to propose new technological methods for assessing the oil and gas prospects of areas of the sea shelf.

2 Background and Related Works

2.1 Studying the Heterogeneous State of the Marine Environment

The first experiments on remote studies of the processes occurring in the layer between the sea and the atmosphere were conducted by Mac Allister with the help of a radiometer developed by him [2]. It was experimentally established that a specific boundary layer with a size of several millimeters and a temperature gradient of several degrees is formed in the surface layer. The temperature from the surface of the water increases linearly to a depth of several millimeters, and then monotonically falls to the temperature of the deep sea horizons. This hydrophysical formation was called the skin layer. The thickness of this boundary layer and the temperature difference between its boundaries mainly depend on the local conditions that determine the flow of heat through the water-atmosphere boundary and the characteristics of turbulence in the upper layer of the sea.

The question of the physical essence of fluid-conducting structures is currently quite complex and ambiguous. First of all, this is due to the entry into the water environment through the atmosphere-water interface of solar radiation and the atmosphere's own radiation. In turn, the water environment forms its own flow of long-wave radiation. In addition, the near-surface layer is affected by convective flows occurring in it, turbulence, internal and surface waves, hydrology, wind effects, evaporation, precipitation, cloud cover, currents, and surfactants.

It is known that hydrocarbons can be discharged into the water environment through fault zones of various geological structures, forming bubbles and mud volcanoes. Gas sources on the seabed are due to significant loosening and high fluid conductivity of rocks, processes of vertical migration of formation and deep, both gaseous and liquid fluids. Under the latter, linear zones of rock densification are considered, which are fixed by distance methods in the form of lineament zones and nodes of their intersection. The movement of formation and deep fluids, which has a discrete or batch mode, in the zone of the geodynamic node, is associated with a change in pressures, both in the fluid-conducting structure itself and in the adjacent zones [3].

Figure 1 shows a diagram of high-frequency sonar of gas “torches” (according to Yevhen Shnyukov). The parameters of gas “torches” depend on the structure of the geofluidodynamic structure, pressure, volume and composition of migrating gases. A high density of gas sources is characteristic of most of the Black Sea, which can be considered as a consequence of active degassing of the subsoil of the region due to the stretching of the lithosphere as a result of mantle diapirism and the processes of the expansion of the planet at the present stage [4].

The mechanism of passage of the migratory flow of hydrocarbon fluids through the water column and its interaction with the water surface is determined by a number of factors, including the type of hydrology, which depends on the season and water area. Figure 2 shows hydrological sections by depth, which were obtained in different water areas and at different times of the year.

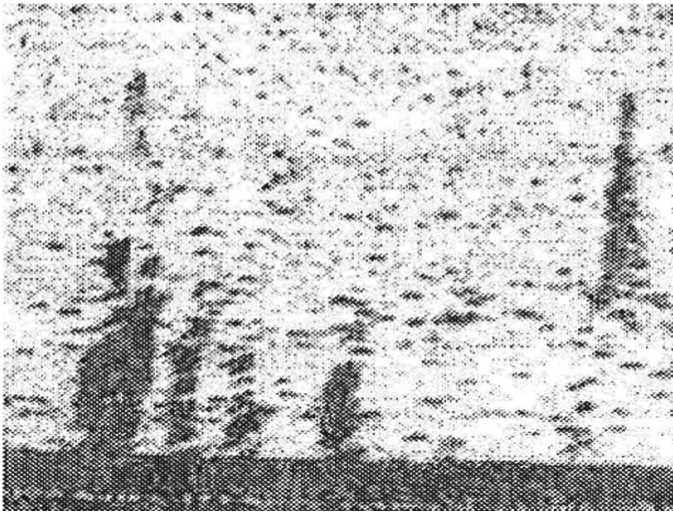


Fig. 1. Diagram of high-frequency sonar of gas “torches”

Figure 3 shows shadow photos of the marine environment in different hydrological conditions. Photographing was carried out using a Tepler camera when the equipment was submerged to a depth of up to 100 m.

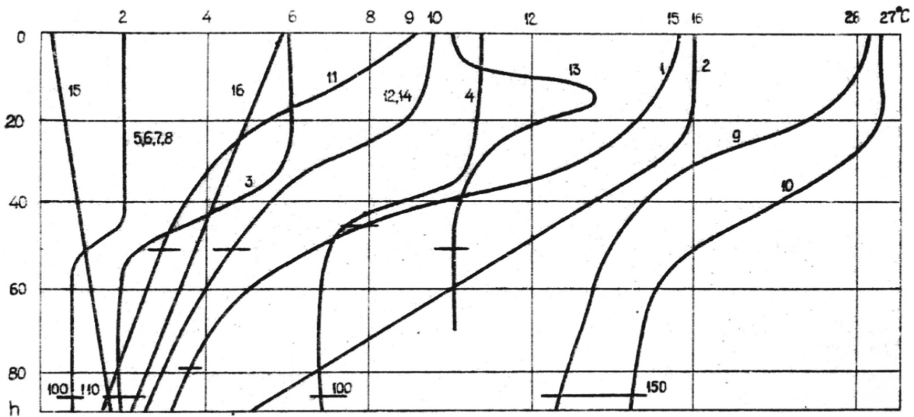


Fig. 2. Hydrological sections by depth, which were obtained in different water areas and at different times of the year

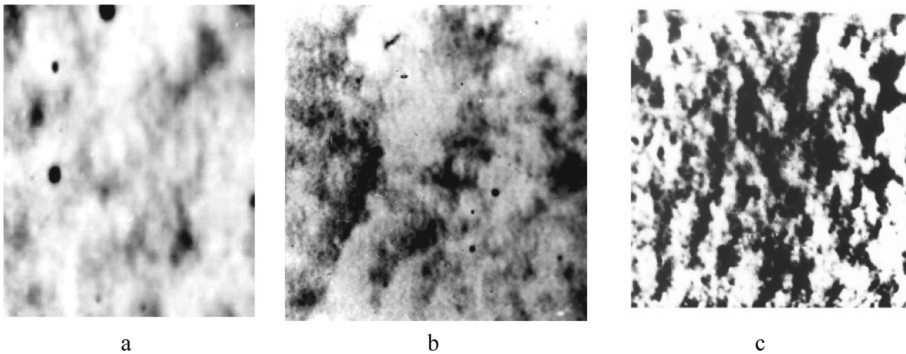


Fig. 3. Examples of different conditions of the marine environment at deep horizons: isotherm or weakly stratified (a), stratified (b), thermocline (c)

2.2 Methods and Results of Studying Specific Temperature Changes

In Fig. 4 provides examples of the state of the marine environment at deep horizons under external excitation, which are noticeably different depending on hydrological conditions, changes in temperature, salinity, underwater currents, the structure of the water environment is different. In the Black Sea, the thermocline is usually located at a depth of about 15–25 m. The disturbance that occurs in it generates density and temperature fluctuations that propagate from the area of disturbance in the form of internal waves (IW).

With hydrology close to isotherm and intense flow of fluids, this can be an airlift process - the rise of cold deep waters to the sea surface by a fluid flow. Secondly, in the presence of density gradients in the stratified water column, migrating fluids also cause the formation of internal waves that propagate to the water surface and interact with it. Thirdly, in hydrology with a pronounced thermocline, the flow of fluids, reaching it,

causes density and temperature fluctuations in it, which spread from the disturbed area to the free water surface in the form of internal waves (IW).

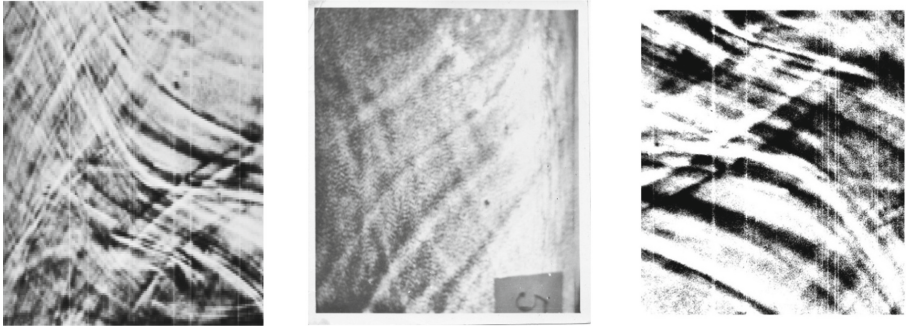


Fig. 4. Examples of shadow images of changes in the texture of the marine environment at deep horizons after external excitation

The frequency of these waves is known as the Brent-Vaisail frequency, and its inverse value (the wave period) serves as the fundamental time scale that determines oscillatory movements in a stratified water medium. The resulting HCs, reaching the water surface, cause changes in the hydrophysical characteristics of the near-surface layer of water, which are reflected on the sea surface as temperature changes, and in the near-surface layer as changes in the temperature gradient. The results of the interaction of emerging deep hydrodynamic processes (DHP) with the near-surface water layer are naturally reflected on the free water surface as temperature anomalies recorded on space images in the infrared spectral range [5].

Figure 5 shows a characteristic temperature profile in the near-surface layer of the liquid [5].

In most cases, under natural conditions, the surface temperature is lower than the temperature below the lying layers of water, which first increases with depth, and then begins to monotonously fall to the temperature of deep horizons. The reason for this phenomenon, with rare exceptions, is that the water surface gives off heat to the atmosphere by radiant and turbulent heat transfer.

To fulfill the condition of heat balance, it is necessary to have a flow compensating for these losses to the surface from the lower water layers. In addition, the near-surface layer is affected by convective flows occurring in it, turbulence, internal and surface waves, hydrology, wind effects, evaporation, precipitation, cloud cover, currents, and surfactants. As a result, an unstable stratification occurs in the surface layer, which can lead to convective movements, the upper layers of water fall into the depth of the liquid, forming cold thermals. The process of formation of such thermals is periodic in nature.

Two forms of free convective flows from the water surface are known: a jet with a spherical front and flows in the form of vertical thermals.

Figure 6 shows the results of laboratory experimental studies of microconvection in the near-surface layer of water with a size of the order of 0.5 cm (shadow photographs of a vertical section of the water surface), in which a dynamic picture of the process

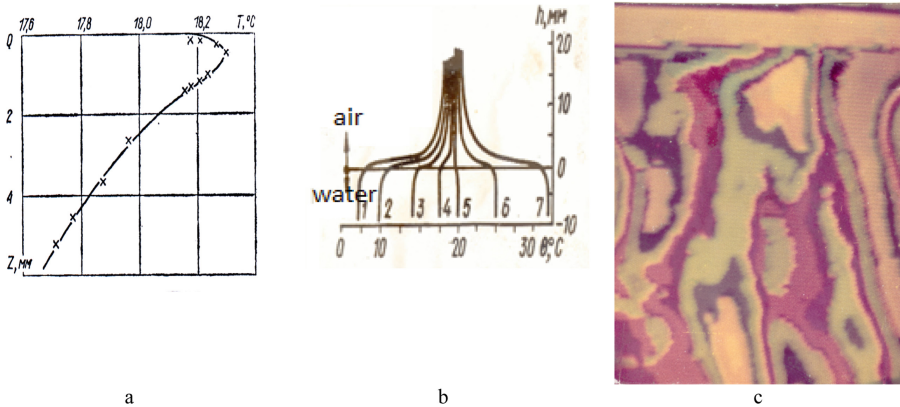


Fig. 5. Characteristic temperature profile in the near-surface liquid layer: a) idealized temperature profile for daytime in summer with weak winds; b) dependence of surface temperature profiles according to Heisler; c) vertical section of the near-surface liquid layer

of formation and development of a cold skin layer near the surface of the water–air separation is presented [6]. The shadow photos show the successive development of cold thermals (1, 2 and 3) in the form of drops breaking off from the water surface. At the same time, areas of increased density are depicted in lighter tones. The formed thermals and their subsequent evolution within 6 s are indicated by dark arrows in the photographs. The speed of movement of the thermals is several millimeters per minute with the size of the thermals of the order of 0.5 cm. In the obtained photos, you can observe the temperature inversion in the upper layer of the studied volume of liquid. At the same time, water cooled by evaporation and radiation “flows” down through these layers, forming a thin surface film. The contrast of the image reflects temperature differences in the near-surface layer, the value of which is proportional to the brightness of the image. Figure shows the formation and movement of cold thermals from the surface into the depth of the liquid during a natural process.

Figure 7 shows shadow pictures of the development of microconvection in the near-surface layer during forced cooling of the water surface. It was found that water in the surface layer is located in thin unstable layers caused by convective processes.

With the appearance of cloudiness, the initial stationary state of the cold laminar layer, ensured by the balance of heat flows, was disturbed. The effective radiation decreased, which caused an increase in the temperature of the skin layer and an increase in evaporation, which is accompanied by the return of heat to the atmosphere. The latter is compensated by the inflow of heat from the homogeneous layer into the cold sublayer before the onset of a new quasi-stationary state caused by the lack of inflow of direct solar radiation. After the passage of the cloud, the temperature of the skin layer remains above its initial state for some time until the complete disappearance of cloudiness, when the thermal parameters of the skin layer begin to asymptotically approach their initial values. Thus, with the appearance of cloudiness, an increase in the temperature of the water surface was recorded and substantiated.

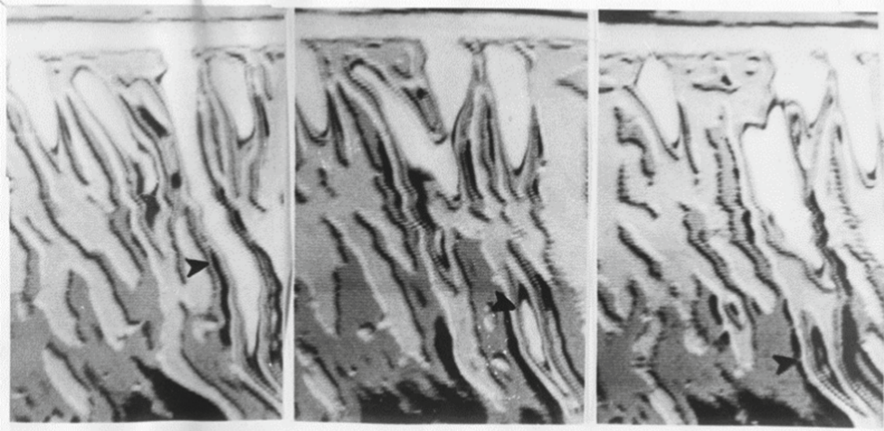


Fig. 6. Results of laboratory experimental studies of microconvection in the near-surface layer of water with a size of the order of 0.5 cm

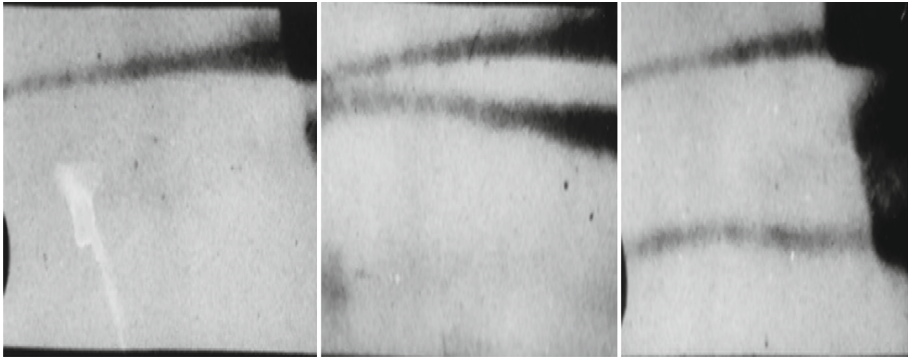


Fig. 7. Results of laboratory experimental studies of microconvection in the near-surface layer of water with a size of the order of 0.5 cm during forced cooling of the water surface

The cold skin is preserved at a wind speed of up to 10 m/s, and the recovery time of the skin layer depends on many external factors. After its destruction due to the collapse of waves and other factors, the recovery time of the skin can be tens of seconds. Therefore, it can be assumed that the existence of a cold skin layer is a rather stable phenomenon.

The volume of water in the thermocline, shifted up or down, will be affected by forces acting in the direction of the reverse shift. Therefore, the perturbation that occurs in the thermocline generates density and temperature fluctuations that propagate from the perturbation region. Convergence and divergence processes caused by internal waves affect the distribution of films of surfactants, oil, and organic liquids that are always present on the surface of the ocean, leading to the formation of characteristic “streaks” that can be seen from the air or from space.

3 Forecasting the Oil and Gas Prospects of Areas Based on Various Characteristics

Analysis of the location of the gas torches on the seabed with the attachment of the latter to the appropriate space images made it possible to determine that they are confined to high-density of liniment and cause thermal anomalies on the sea surface, which certify the presence and hydrocarbon deposits. The physical basis of the formation of geo-infection features of underwater landscapes is the transmission of information on the intensity of the stress-deformed state of the lithosphere and fluidogeodynamic processes passing from depth to the earth's surface [7].

Direct and indirect geoindicative signs of underwater landscapes are distinguished. Direct signs are related to the physiognomic features of underwater landscapes, which shine through everywhere in the water column. Indirect geoindicative features associated with hydrodynamic processes occurring in the water column and on the surface of the sea, where the main role is played by the hydrological and hydrophysical factor.

Thus, in shallow water conditions, the neotectonic active structure associated with the Schmidt field (Fig. 8) is clearly visible in the relief of the seabed, where the lighter phototone corresponds to the area in the relief located above the Schmidt field. This is triggered by the neotectonic factor in the formation of an optical anomaly on the aerospace image of the sea surface, through the thickness of the water the light rocks of the seabed.

Figure 9 shows a fragment of a space image of the northwestern shelf of the Black Sea (NOAA satellite channel 4 (10.3–11.3 μm)) from the temperature anomaly over the Golitsyn hydrocarbon field (according to O.Yu. Kotlyar). From Fig. 9 we see that there are both cold (black spots) and warm (light spots) anomalies on the sea surface, that is, it can be assumed that both processes of surface temperature anomaly formation are present: bubbles and internal waves [8] (Tables 1 and 2).

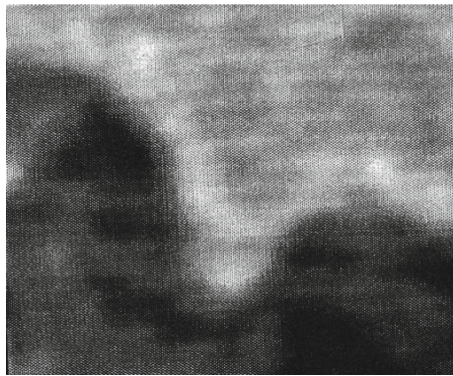


Fig. 8. Fragment of a space image of an optical anomaly over the Schmidt hydrocarbon deposit

Table 1. The value of the Haralik parameters over the Schmidt hydrocarbon deposit

Haralik parameters	Anomaly	Background
1. Contrast	1133	155
2. Sum Variance	8,1	0,8
3. Sum Entropy	0,12	0,08
4. Entropy	13,9	5,0
5. Difference Entropy	0,7	0,5

**Fig. 9.** Temperature anomaly over the Golitsyn hydrocarbon deposit. (according to O. Yu. Kotlyar)**Table 2.** Values of Haralik parameters over the Golitsyn hydrocarbon deposit

Haralik parameters	Anomaly	Background
1. Contrast	4,88	0,01
2. Sum Variance	288	0,37
3. Sum Entropy	4,24	0,41
4. Entropy	5,18	0,42
5. Difference Entropy	1,93	0,08

In this connection, interest arose in researching the mechanism of formation of optical anomalies and hydrothermal processes that occur at the boundary of the sea surface-atmosphere separation for the subsequent use of the results of theoretical studies in the development of methods for deciphering space images and detecting oil and gas deposits.

The surface of the sea and the boundary layer of the atmosphere adjacent to it are in a close thermal and dynamic interaction, which occurs through radiant and contact heat transfer, as well as evaporation.

For a near-surface layer of water of the order of 1 cm (with tolerances), the heat balance equation has the form:

$$q = R + Q + i, \quad (1)$$

where R is the balance of long-wave radiation; Q - contact heat exchange of the sea surface with the atmosphere; i - heat consumption for evaporation.

In connection with the difficulties of determining the total heat flow by means of calculations, in practice, the method of its direct measurement along the temperature gradient is used [9].

$$q = kd/dZ, \quad (2)$$

k is the coefficient of thermal conductivity of the near-surface skin layer of water Z .

The value of k is easily calculated within the upper two-centimeter layer of water

$$k = k_0(1 + vZ), \quad (3)$$

k_0 is the molecular value of the thermal conductivity coefficient ($Z = 0$), v is the rate of change of k (600 m⁻¹).

Therefore, the task of determining the total heat flow from the sea surface is reduced to measuring the temperature gradient in the surface layer of water.

The water surface - atmosphere system is modeled by the liquid - vapor system, the thermodynamic equilibrium between which is disturbed by external radiation. A heat-conducting liquid obeying the Navier–Stokes law is chosen as a model. The complexity of the mathematical description lies in the task of non-equilibrium boundary conditions that must be satisfied by the hydrothermodynamic parameters of the two media. There are a number of temperature boundary layer models. However, all of them are based on the assumption that its destruction occurs periodically and the influence of phase transitions on the structure of the thermal boundary layer is not taken into account.

In a number of cases, it is possible to obtain a pronounced dependence of the effective radiation depth Z_{ef} and the thermal state of the water. The mathematical model for Z_{ef} after a number of transformations looks like this

$$Z_{ef} = \frac{\int_{\lambda_1}^{\lambda_2} \varepsilon(\lambda)(dm_{eS}/dZ)\alpha e(\lambda)^{-1}d\lambda}{\int_{\lambda_1}^{\lambda_2} \varepsilon(\lambda)(dm_{eS}/dZ)d\lambda}, \quad (4)$$

where $\varepsilon(\lambda)$ is the spectral emission coefficient, m_e is the energy luminosity of the black body, $\alpha e(\lambda)$ is the spectral absorption coefficient.

To calculate the effective depth of radiation in the case of a narrow spectral interval, H. Macalister derived the following expression for Z_{ef} .

$$Z_{ef} = 1/\alpha e(\lambda), \quad (5)$$

Thus, for the spectral intervals of 2.0–2.4 μm and 3.5–4.0 μm , the depths at which the temperature was measured are 0.5 mm and 0.06 mm, respectively.

By successively measuring the radiation of water in different spectral ranges, it is possible to determine the water temperature at different depths and, as a result, knowing the

value of Z_{ef} , calculate the temperature gradient. The latter can be used as an informative sign of the presence of hydrocarbon deposits during space remote sensing monitoring of the shelf zone of the Azov-Black Sea basin and determination of temperature gradient anomalies in the near-surface layer of the sea surface.

For a further detailed study of the process of formation of temperature anomalies on a free water surface, the results of an experiment previously performed at different times in the Black Sea from the ship OS-6 (Fig. 10), as well as continued in the Barents Sea and the Sea of Japan, were used. Modeling was performed by disturbing the deep horizons with the help of a submerged self-propelled model (as a simulator of hydrocarbon deposits), and the registration of emerging anomalies was carried out as a result of their sequential crossing by a ship with optical highly sensitive scanning equipment with parameters: spectral range 3.5–5.2 μm , spatial resolution on the water surface is 1–2 m.



Fig. 10. A ship with an installed thermal imager

Figure 11 shows fragments of an IR image of the temperature background of the sea surface (a) and temperature anomalies disturbed on the water surface (b, c, d, f) by a submerged mobile model and obtained as a result of their successive crossing by the ship as the anomalies develop from 30 min (b) up to 3 h (f) respectively.

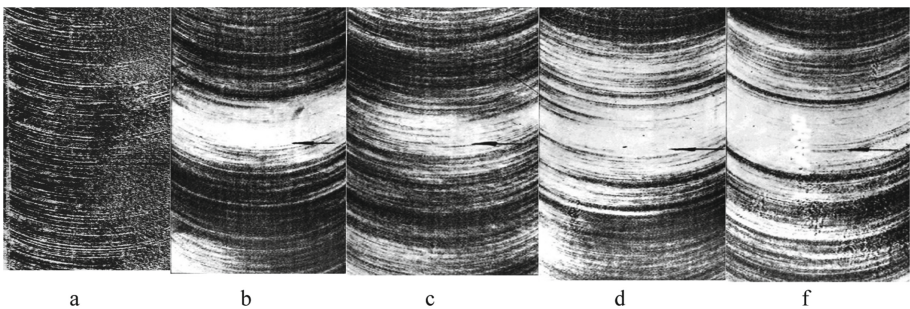


Fig. 11. Fragments of an IR image of the temperature background of the sea surface (a) and temperature anomalies on the water surface (b, c, d, f)

Arrows in Fig. 11 shows the direction of movement of the hydrodynamic process model. The arc-shaped image of temperature anomalies is related to the relationship between the scanning speed and the speed of the ship carrying the thermal imager.

The obtained IR images of anomalies were processed to obtain informative features of the background and signal. For this, the structural and textural characteristics of the water surface were used by calculating the values of the Haralik parameters from infrared images (Fig. 11). Entropy (H) was determined as the most informative parameter of Haralik [10].

$$H = \sum_{i=1}^N \log(1/p_i) \cdot p_i, \tag{6}$$

where, p_i is the probability of a pixel value of a digital image, $i = 1 \dots N$ is the number of a pixel value of a digital image (Fig. 12).

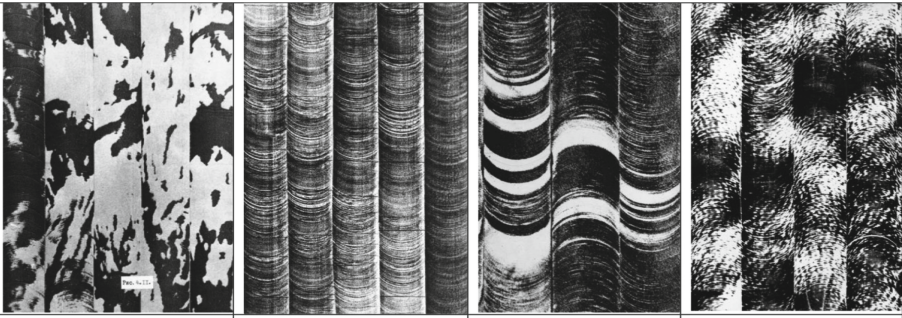


Fig. 12. Temperature anomalies on the surface of the Black, Barents, Japanese and Mediterranean seas

Table 3. Value of entropy at different times of development of temperature anomalies on the water surface by the submerged moving hydrodynamic process model

Images	a	b	c	d	f
Time of development of anomalies	background	30 min	1.5 h	2 h	3 h
Entropy	8,21	8,68	8,82	8,86	8,92

Table 3 shows that the background has a minimum entropy value, and with the appearance of an anomaly and the life time of the anomaly, the entropy value increases to the maximum value, after which, as the temperature wake of the model dissipates, it begins to fall to the background values.

where

$$p(i, j) = \frac{x(i, j)}{\sum_{i=1}^N \sum_{j=1}^N x(i, j)}$$

$$\mu_{x+y} = \sum_{k=2}^{2N} k \times p_{x+y}(k)$$

Table 4. Haralik parameters and corresponding formulas

N	Sings	Formulas
1	Contrast	$\sum_i \sum_j (i - j)^2 p(i, j)$
2	Sum Variance	$\sum_{k=2}^{2N} (k - \mu_{x+y})^2 p_{x+y}(k)$
3	Sum Entropy	$-\sum_{k=2}^{2N} p_{x+y}(k) \log p_{x+y}(k)$
4	Entropy 1	$-\sum_{i=1}^N \sum_{j=1}^N p(i, j) \log p(i, j)$
5	Entropy 2	$-\sum_{k=0}^{N-1} p_{x-y}(k) \log p_{x-y}(k)$

$$p_{x+y}(k) = \sum_{i=1}^N \sum_{j=1}^N p(i, j), i + j = k$$

$$p_{x-y}(k) = \sum_{i=1}^N \sum_{j=1}^N p(i, j), |i - j| = k$$

As a result of the retrospective analysis and processing of archival materials of physical modeling of the process of formation of temperature anomalies of natural and man-made origin on the water surface, several dozen different parameters of Haralik were checked and the five most informative of them were selected for further use: Contrast, Sum Variance, Sum Entropy, Entropy, Difference Entropy (Table 4).

A comprehensive method of prediction of oil and gas perspective areas on shelf is tested, which, taking into account the geological features of the bottom of the marine shelf, consists of four stages [11].

At the first stage of the research, visual contrast-analog decoding of space images is performed, which is based on the property of remote data to reflect the deep geological structure. At the second stage, structural and geomorphological studies of the bottom relief are carried out based on the analysis of bathymetric and geomorphological maps and their transformations. This stage consists of numerous methods of analyzing the modern topography of the bottom in order to highlight anomalies in the structure, which are geoindicators of deep faults and blocks active at the latest tectonic stage, and to determine the relative neotectonic activity of the latter. To assess the relative neotectonic activity of the blocks, morphometric constructions (maps of horizontal and vertical dismemberment, gradient zones) are carried out; data on the modern geodynamics of the surrounding land, analysis of modern sediment accumulation and granulometric composition of bottom sediments are included. The comparative tectonic analysis is carried out at the third stage. The basis of this analysis is the visual comparison of the obtained analytical maps with a priori geological and geophysical information. Lineaments are identified with tectonic faults and disturbances in the sedimentary cover revealed by geophysical data, classification of lineament zones into confirmed and unconfirmed ones is carried out. By the comparison method, an analysis of the ratio of structural plans of the Meso-Cenozoic is carried out and structures with inherited development are revealed. In

automatic mode, by integrating remote sensing data and geological-geophysical data, an analysis of the heredity of the territory's development is performed [12]. At the fourth stage, an assessment of the oil and gas prospects of areas of the sea shelf is carried out on the basis of neotectonic, structural-geomorphological, structural-geological criteria. Further analysis consists of determining the rank of oil and gas prospective areas according to the main characteristics obtained by decoding of space images, neotectonic and morphometric analysis, structural and tectonic data. The characteristics of each zone are compiled taking into account the rank of oil and gas prospective areas, which were evaluated by rating according to a set of criteria. Establishing a priority rating is the basis for determining the priority areas for exploration for oil and gas.

The main factors affecting the formation and redistribution of oil and gas deposits are geofluidodynamic and neotectonic. The result of the action of these deep processes is manifested in the contours of the modern relief and landscape as a whole. Thus, when identifying zones promising for oil and gas on the sea shelf, there is a study of geofluidodynamic processes and neotectonic movements. Geofluidodynamic processes due to the impact on landscapes, water environment and sea surface are quite clearly recorded on remote sensing materials as temperature anomalies.

In the proposed method of assessing the oil and gas prospects of areas on the sea shelf [13], as an additional informative sign of hydrocarbon deposits, changes in the temperature gradient of the near-surface layer of water under the influence of hydrocarbon fluids are used by calculating the values of radiation values in two spectral ranges (far and near infrared) based on the data of multispectral space surveys, then calculate the effective radiation depth for the given spectra and, based on the obtained data, determine the radiation gradient in the near-surface layer of water, compare the calculation results with the parameters of the reference areas, and make a predictive assessment of the presence of gas deposits.

In order to increase the probability of prediction and the effectiveness of the search for explosives, as an additional informative sign of the presence of explosive deposits, use changes under the influence of hydrocarbon fluids of structural and textural parameters, namely "entropy". The novelty and physical essence of the proposed method is that the structural and textural features of temperature anomalies allow calculating the size, shape, orientation of the relative location of the spatial component images of temperature anomalies. The increase in the probability of prediction and the effectiveness of the search for explosives is due to the fact that the structural-textural feature on the sea surface is a more stable unmasking informative feature, which, despite seasonal weather variability, maintains a qualitative and quantitative assessment throughout the time of searching for explosives. To substantiate the proposed method, modeling of the formation of temperature anomalies on the water surface in the experimental basin was performed, which confirmed the information content of the function of "entropy" to decipher optical anomalies on the images of the water surface.

4 Modeling by the Method of Analytical Networks

To determine the most promising oil and gas area, mathematical modeling was applied by creating a corresponding mathematical model. As an example, consider the model (Fig. 13), created on the basis of the analytical network method (ANM) [14].

The choice of this method is due to the fact that ANM allows you to process more diverse and complex structures taking into account the dependencies between levels and feedback between level elements, thereby achieving greater objectivity and reliability in decision-making. On the basis of ANM, the problem is structured in the form of a network model, on the basis of which the relationships between the proposed alternatives and the generalized criteria for choosing the most promising oil and gas site are determined. For this purpose, three search areas (# 1, # 2 and # 3) of the Caspian shelf of Turkmenistan were selected, which received the highest score at the first stage according to the objective function.

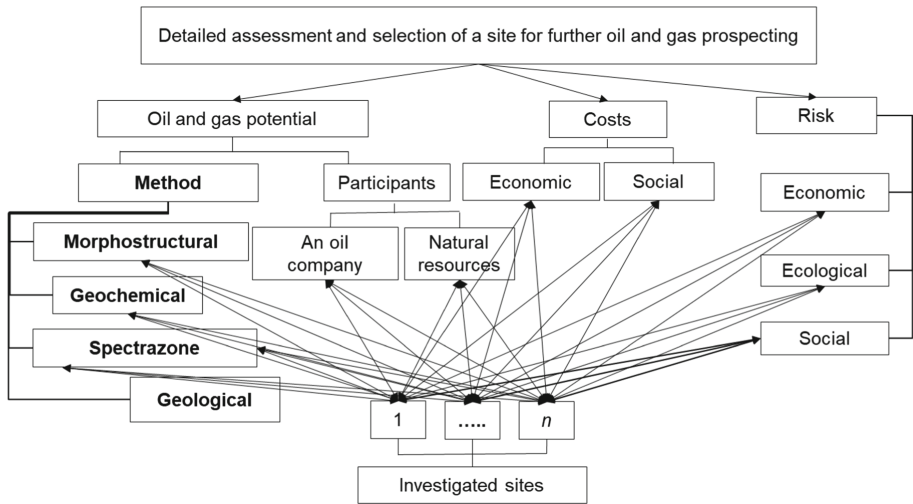


Fig. 13. Network model of relationships between proposed alternatives and generalized selection criteria for determining the most promising oil and gas area

On the created network model and interpretation of the results, calculations conducted on the basis of the Super Decision software product (SP) were performed. Calculations were carried out in three stages:

Step 1. Experts in the field of the subject are determined the priorities by which each of the three regions will be evaluated. The assessment was carried out on an intensity scale from 1 to 9.

Next, in the SP Super Decision, relationships between criteria and alternatives are built and expert evaluations are made for each.

Step 2. The supermatrix and the limit matrix of the elements of relationships are calculated. The most promising oil and gas areas are determined according to separate generalized criteria ("Oil and gas prospects", "Costs", "Risks").

Step 3. Depending on the task, in our case, it is an assessment of the oil and gas potential of prospective areas, a formula is determined, according to which the final calculation will be carried out taking into account the generalized criteria and expert assessments based on the priorities of the selected criteria. In this case, the standard additive (probabilistic) formula was used.

As a result of a detailed study based on the ANM and according to the final ranking data, the following estimates of the oil and gas prospects of three selected areas of the Caspian shelf of Turkmenistan were obtained: # 1–0.31; #2–0.39 and #3–0.30.

5 Conclusion

1. Hydrophysical processes occurring in the near-surface layer of water are caused primarily by the entry into the water environment through the atmosphere-water separation of solar radiation and the action of hydrocarbon fluids that create bubbles and internal waves, which are reflected on the sea surface by the appearance of temperature anomalies that are registered in optical (infrared) range.
2. Between the hydrophysical and hydrodynamic processes in the near-surface layers of water at the water-atmosphere interface, on the one hand, and fluid-dynamic processes, the geological structure of the lithosphere, and underwater landscapes, on the other, there is a relationship that must be taken into account when detecting hydrocarbon deposits based on remote sensing space shooting.
3. Important factors and conditions for obtaining high-quality space images of the sea shelf for effective search for hydrocarbons are the time and season of shooting, cloud cover, sea temperature, presence of wind and fog, density of phytoplankton and salinity of sea water.
4. A mathematical model created on the basis of the analytical networks method (ANM) is used to determine the most oil and gas -perspective area. As a result of a detailed study on the basis of ANM and, according to the final ranking data, the assessments of oil and gas per prospection of the three selected sections of the Caspian shelf of Turkmenistan were obtained.

References

1. Lyalko, V.I., Popov, M.O., Fedorovskyi, O.D.: Multispectral methods of remote sensing of the Earth in nature management problems, Kyiv, Naukova dumka (2006)
2. Mc Alister, E.D. Measurement of total heat flow from the sea surface. *Appl. Opt.* **5b**, 188–201 (1964)
3. Break, V.M., Pererva, V.M., Kostyna, T.I.: Geofluid dynamic structures of the lithosphere and diapirism. *Rep. NAS Ukraine* **2**, 131–136 (2002)
4. Shnyukov, E.F., Starostenko, V.Y., Kobelev, V.P.: Geological studies. *Geof. J.* **26(4)**, 116–132 (2004)
5. Akimov, E.A., Stanichny, S.V., Polonsky, A.B.: Using SEVIRI scanner data to estimate the temperature of the surface layer of the Black Sea. *Mor. Hydrophys. J.* **6**, 37–46 (2014)
6. Fedorovsky, A.D., Nikyforovych, E.I., Prykhodko, N.A.: Transport processes in gas-liquid systems, Kyiv, Naukova dumka (1988)
7. Kolodiy, V.V., Kolodiy, I.V.: Fluid dynamics of the shelf part of the North-Black Sea oil and gas-bearing basin. *Geol. Ukraine* **1**, 41–44 (2004)
8. Fedorovskyi, O.D., Khyzhniak, A.V., Filimonov, V.Y.: Justification of the dual-use of aerospace geomonitoring of the offshore shelf: exploration of hydrocarbon deposits and “highlighting” the marine situation. *Space Sci. Technol.* **27(129)**, 38–44 (2021)

9. Nikyforovych, E.I., Fedorovsky, O.D.: Hydrothermodynamics of the near-surface liquid layer. *Visn. Acad. Sci. Ukrainian SS* **11**, 15–21 (1984)
10. Haralick, R.M.: Statistical and structural approaches to texture. *Proc. IEEE* **67**(5), 786 (1979)
11. Yefimenko, T.A., Sedlerova, O.V.: Geoinformative signs of neotectonic processes in the Azov-Black Sea region, problems of geodynamics and oil and gas carrying capacity of the Black Sea-Caspian region. In: 5th International Conference “Crimea-2003”, 8–13 September, pp. 269–272 (2003)
12. Sedlerova, O.V.: Geological interpretation of the data integration multispectral satellite imagery and geological and geophysical data for predict oil and gas zones at the regional level (in the example of the north west shelf of the Black sea). *Ukr. J. Remote Sens.* **7**, 47–57 (2015)
13. Patent of Ukraine No. 108696, Lyalko V.I., Fedorovsky O.D., Yakymchuk V.G., Sokolovska A.V., Vorobyev A.I. Method of forecasting gas deposits on the sea shelf. 05/25/2015
14. Saati, T.: *Decision-Making with Dependencies and Reverse Connections: Analytical Networks*. Librokom, Moscow (2009)